ENGINEERING RESEARCH INSTITUTE
UNIVERSITY OF MICHIGAN
ANN ARBOR

WIDE-BAND AMPLITUDE DISTRIBUTION ANALYSIS OF VOLTAGE SOURCES

Technical Report No. 22
Electronic Defense Group
Department of Electrical Engineering

By: L. W. Orr

Approved by: H. W. Welch, Jr.

Project M970

TASK ORDER NO. EDG-7
CONTRACT NO. DA-36-039 sc-15358
SIGNAL CORPS, DEPARTMENT OF THE ARMY
DEPARTMENT OF ARMY PROJECT NO. 3-99-04-042
SIGNAL CORPS PROJECT NO. 29-194B-0

October, 1953

TABLE OF CONTENTS

LIST OF FIGURES

ABSTRACT

This report describes a method of wide-band amplitude distribution analysis employing two commercial oscilloscopes and a phototube. A minimum set-up can be assembled in two hours from available laboratory equipment which is accurate to about 5%, and performs the analysis in 5 seconds. It is free from the severe bandwidth restriction of other methods, and can often be employed up to 500 mc. A full discussion of the technical details is given, and results on various noise sources are included for illustration. A modification of the minimum set-up for improving the resolution and and increasing the accuracy is presented.

WIDE-BAND AMPLITUDE DISTRIBUTION ANALYSIS OF VOLTAGE SOURCES

1. INTRODUCTION

A method of obtaining a semiquantitative amplitude distribution analysis is very useful in studies of certain voltage sources such as random noise sources. Desirable properties of such a method include the use of only equipment which is readily available in the laboratory, simplicity of the set-up, speed of analysis, reasonable accuracy and wide bandwidth. For the method described in this report, only two oscilloscopes, one phototube and a few small parts are required for the minimum set-up, which can be assembled in two hours. The amplitude distribution density function is displayed as an oscillogram which can be recorded photographically in 5 seconds. The accuracy of analysis is better than 5% under most conditions, and may be improved by a more elaborate set-up discussed in Section 8. The bandwidth of the system is determined by the vertical amplifier of the A-scope, but under certain conditions the bandwidth may be extended to 500 mc.

An elaborate system for experimental noise analysis was developed at MIT, and is described by Knudtzon.[1] Although capable of high precision, this system is greatly restricted in bandwidth, and the time required for a particular analysis is quite long.

---

[1] Knudtzon, "Experimental Studies of the Statistical Characteristics of Filtered Random Noise," Research Laboratory of Electronics, MIT Technical Report No. 115, July 15, 1949.

A phototube scanning method of analysis was suggested by D. F. Winter[1] affording speed and flexibility without any great accuracy, but no further mention of this is found in the literature. The present report gives a full discussion of the principles involved, the details of adjustment and the limitations of the method.

2. BASIC CONSIDERATIONS

2.1 Probability Distribution, P(y)

Consider a voltage source whose amplitude may be expressed by a discrete function of time.

$$y = f(t) \quad . \tag{1}$$

The probability distribution or amplitude distribution function P(y) of the source is the probability of finding an amplitude larger than y at any given instant. This is identical with the ratio of the time spent above y to the total time if the observing interval is arbitrarily long.

As a simple example, let us first examine a normalized sine voltage.

$$y = \sin \omega t \quad . \tag{2}$$

The probability distribution is found by calculating the fraction of total time that the function exceeds amplitude y. It is given for the sinusoid by the relations

$$\left.\begin{aligned} P(y) &= 1 \ , & y &< -1 \\ P(y) &= x/\pi \ , & -1 &\leq y \leq 1 \\ P(y) &= 0 \ , & y &> 1 \\ \text{where } x &= \cos^{-1} y \ , & 0 &< x < \pi \end{aligned}\right\} \tag{3}$$

[1] Ibid., p. 17.

The probability distribution also exists for a voltage source whose output cannot be predicted as a discrete function of time, such as random noise. However if the source is consistent, its probability distribution function may be assumed to be the value calculated from past performance.

2.2 Probability Density, p(y)

The probability density function is the negative derivative of P(y) and may be expressed by the relation

$$p(y) = \lim_{\Delta y \to 0} \frac{P(y) - P(y + \Delta y)}{\Delta y} \quad . \tag{4}$$

This is frequently a more useful quantity in amplitude distribution analysis. For the sinusoid, the following relations hold for p(y).

$$\left.\begin{aligned} p(y) &= 0 \quad , \quad y < -1 \\ p(y) &= \frac{1}{\pi\sqrt{1 - y^2}} \quad , \quad -1 < y < 1 \\ p(y) &= 0 \quad , \quad y > 1 \end{aligned}\right\} \tag{5}$$

Plots of relations (3) and (5) are shown in Fig. 1. It is seen that as y approaches 1 or - 1, p(y) approaches an infinite value.

2.3 Incremental Probability Density, $p_\Delta(y)$

In attempting to design equipment for measuring p(y) we at once face the difficulty of measuring quantities which approach zero, and ratios which in some cases approach infinity. It becomes necessary to compromise on a finite Δy and an <u>incremental probability density</u> $p_\Delta(y)$ defined by the relation

$$p_\Delta(y) = \frac{P(y - \frac{1}{2}\Delta y) - P(y + \frac{1}{2}\Delta y)}{\Delta y} \quad . \tag{6}$$

M-970 A-S4-47 JEM 10-7-53

FIG. 1

PROBABILITY P(y) AND
PROBABILITY DENSITY p(y) OF A SINUSOID.

2.4 Resolution

The smaller we are able to make Δy in our analyzer, the more closely does $p_\Delta(y)$ approach the probability density, $p(y)$. The resolution is thus improved as Δy is decreased. It is convenient at this point to introduce the following terms:

$$\underline{\text{Unit Resolution}} = \Delta y \tag{7}$$

$$\underline{\text{Peak Resolution Index}}, R_p = Y/\Delta y \tag{8}$$

where $Y = (y_{max} - y_{min})$, the peak to peak voltage of the source.

In dealing with certain sources having large but infrequent peak amplitudes, this index is not convenient. In such cases an rms index may be adopted.

$$\underline{\text{RMS Resolution Index}}, R_{rms} = \sqrt{\overline{y^2}} \Big/ \Delta y \quad . \tag{9}$$

2.5 $p_\Delta(y)$ for a Sinusoid

For the sinusoid, we may calculate the incremental probability density for $R_p = 20$. This function is plotted in Fig. 2A. Results of sinusoid analysis using the equipment to be described appear as oscillograms, Fig. 2B and C. The value of R_p in the equipment was also 20. Fig. 2B is for a 10 megacycle sine wave, while Fig. 2C is for a 10 kilocycle sine wave of equal amplitude, showing the expected identical distribution. The width of the central pulse in Fig. 2B is a measure of the Unit Resolution.

3. METHOD OF ANALYSIS

The method used in making incremental probability density analysis is based on two physical principles. The first principle deals with the action of a phosphor in responding to variations of electron density. The second principle deals with the integrating action of a phototube and capacitor.

A. CALCULATED

B. OBSERVED ON 10 MC SINE WAVE.

C. OBSERVED ON 10 KC SINE WAVE.

FIG. 2

INCREMENTAL PROBABILITY DENSITY FOR A SINUSOID.

3.1 Phosphor Response

It is found by experiment that under certain easily realized conditions, the light output from a phosphor is linear with the electron density received. Furthermore, the integrated light output per sq. cm. of a phosphor is also linear with the integrated current density over a wide range of pulse rates. The conditions under which this linearity of response is obtained are as follows:

(1) The instantaneous current density does not exceed the steady state linear response region of the phosphor, or

(2) If it does exceed this density at any instant, the phosphor is of sufficiently short persistence that excitation in any small unit area is sufficiently infrequent so that "saturation buildup" is avoided.

The physical situation under these conditions is simply that there exists always an adequate supply of unexcited action centers in the phosphor to be offered to incoming electrons. A tube with a short persistence phosphor is therefore employed in the apparatus.

3.2 Phototube Integration

The emitted photocurrent for a photo-sensitive surface is linear over a large range of illumination. If an adequate electric field is applied, there will be no space charge limiting, and all the photoelectrons will be collected at the phototube anode. Photocurrent is thus made practically independent of anode voltage as is illustrated by Fig. 3A. Because of this fact it may be easily proved that in the circuit of Fig. 3B, the voltage across capacitor C is almost exactly equal to the average photocurrent. This holds for an a averaging interval t, provided that $RC >> t$, and that steady state conditions have been established.

A. ANODE CHARACTERISTIC

B. INTEGRATOR CIRCUIT.

FIG. 3

IP42 PHOTOTUBE INTEGRATOR.

3.3 Scanning Method

The voltage to be analyzed is displayed in the usual manner on a short persistence CRO called the A-scope (analyzing oscilloscope). If we were to scan the image slowly with a vertically moving slit and integrating phototube, the resulting output signal would produce the function $p_{\Delta}(y)$.

Two disadvantages are inherent in this method. First, it involves a mechanical scanner requiring accurate machining. Second, the response of the phosphor is somewhat variable over the surface giving substantial errors in measurement.

We may avoid both difficulties by keeping the slit and phototube fixed in position. Now the same area of phosphor will be used throughout the measurement. Scanning is accomplished by a vertical motion of the entire pattern over the face of the A-scope. A convenient method of manual scanning is furnished in the vertical centering control.

The integrated phototube output may be displayed on the Y-axis of a second CRO called the D-scope (display oscilloscope). The X-axis signal for the D-scope must be synchronized with the vertical scanning motion of the A-scope to produce accurate oscillograms.

4. APPARATUS

4.1 Minimum Set-Up

The minimum set-up for amplitude distribution analysis is illustrated in Fig. 4. In a later section, a more elaborate set-up will be described, but the present set-up is quite adequate for most analyses as is demonstrated by Fig. 2.

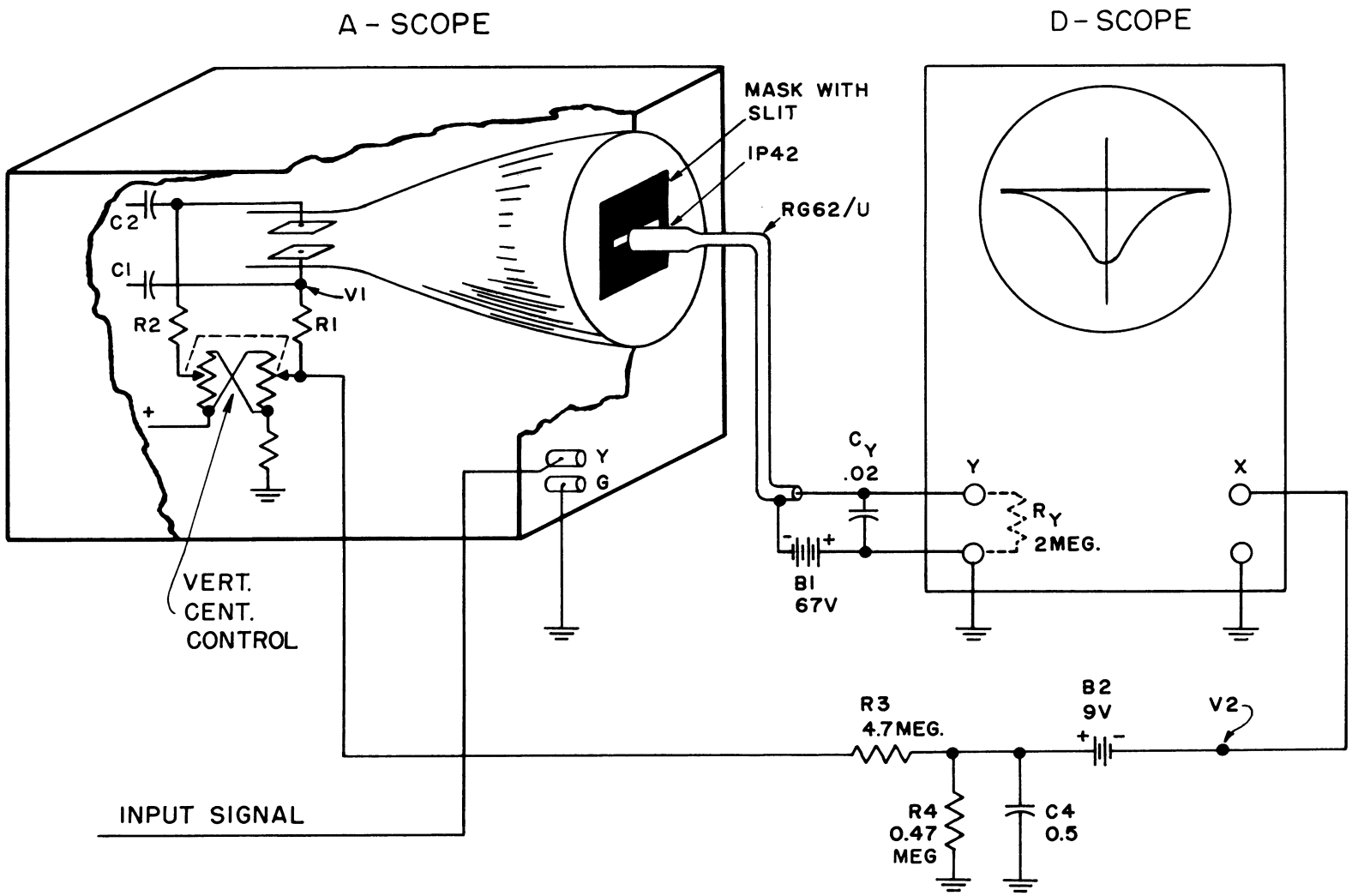

FIG. 4

MINIMUM SET-UP FOR ANALYZER.

4.2 Oscilloscopes

The requirements for the A-scope are as follows. It must be equipped with a CRT having a P5 or P11 phosphor. It must be free of vertical drift, and for this reason an ac amplifier is preferred. The vertical amplifier must be of adequate bandwidth for the signal to be analyzed. However, if the signal is of sufficient amplitude, it may be coupled directly to the vertical deflection plates. In this case the only inherent limitation in bandwidth is the transit time of the electron beam.

If the deflection region has an axial length of 2.5 cm and the beam energy at deflection is 2 kv, the transit time (during deflection) will be approximately one millimicrosecond permitting operation up to 500 mc.

The requirements for the D-scope are quite different. The vertical amplifier will ordinarily operate at maximum gain, and a large gain is required (at least 50 mv/inch). It must have direct coupled X and Y amplifiers both as free from drift as possible. The frequency response of the amplifiers is unimportant, as the signals applied will be generally below 1 cps. A high input impedance is desirable for the Y input. The Tektronix 512 or Dumont 304H are both suitable for this application. The former is preferred because of its greater freedom from drift at maximum gain, the latter because of the larger input impedance (2 megohms), and high gain (30 mv/inch).

4.3 Phototube

The 1P42 phototube was chosen for its construction, and relatively large sensitivity (30μa/lumen). At low light levels, it has the desired flat characteristic shown in Fig. 3B, and has a very small dark current (less than 10^{-9} amp). In operating the apparatus, the usual maximum level of light entering the tube was 10^{-3} lumen. This produced a current of 30×10^{-9} amp

giving a 60 mv signal in the 2 megohm load resistor. The vertical deflection factor of the D-scope was 30 mv/inch at maximum gain, resulting in a 2 inch deflection of the beam.

4.4 Details of Assembly

Returning to Fig. 3, the central portion of the A-scope face is masked with 3M No. 33 electric tape except for a small central slit 1 mm high and 8 mm wide. The horizontal edges of the slit are lined up parallel with the horizontal trace. The body of the phototube is shielded by a slightly expanded section of RG 62/U coaxial cable. The copper shield is connected to the cathode sleeve, and the central wire to the anode. The tube is supported so that its window is centered on and touching the slit.

Integrating capacitor C_y is chosen large enough to smooth the 60 cycle intensity ripple usually found in oscilloscopes with unregulated accelerating voltages. This value of C_y was adequately large to produce satisfactory integration of all signals analyzed. The dc input resistance, R_y of the D-scope is employed as the phototube load, and voltage is furnished from a small 67-volt battery B_1.

If the room illumination is large, the face of the A-scope will require shielding to prevent light leak. Since it is an advantage to be able to see a portion of the A-scope trace in making adjustments, a darkened room is preferred.

The X input of the D-scope is furnished by a voltage V_2 in Fig. 3. The coupling circuit is arranged so that upon turning the vertical centering control, voltages V_1 and V_2 will stay in synchronism.

The circuit requirement for this may be stated by the relation

$$R_1 C_1 = \frac{R_3 R_4 C_4}{R_3 + R_4} \quad . \qquad (10)$$

Battery B_2 eliminates a large portion of the dc component, so that the horizontal centering control of the D-scope may operate normally.

5. OPERATION

The horizontal sweep of the A-scope is adjusted for some sweep frequency near 100 kc which is asynchronous with any frequency component in the input signal. The horizontal synchronism is set at zero. A sweep length of about one inch is generally satisfactory in satisfying the requirements in Section 3.1. Before applying the input signal, both scopes are centered in the usual way. The size of the resolution pulse may be observed by slowly moving the vertical centering control of the A-scope with its Y-input shorted.

To plot the $p_{\Delta}(y)$ function, the input signal is applied to the A-scope and appropriate gain adjustment made so that the signal nearly fills the vertical dimension,but without overloading the amplifier. This last precaution is unnecessary if the input signal is direct-coupled to the A-scope deflection plates.

The vertical centering control of the A-scope is now turned slowly (in 5 seconds) from one extreme position to the other. It becomes the manual scanning control. During scanning, an oscillogram may be made by a time exposure on the D-scope. If a base line is desired, a second exposure may be made of one scan with the Y-input of the D-scope shorted. It is important here to check drift in the D-scope.

There is one distinct advantage in the manual-controlled scan for recording. It is this. The spot on the D-scope may be made to move at almost constant velocity regardless of the shape of the curve. The result is a clear oscillogram of constant line width and density.

6. SYSTEM RESOLUTION

Figure 5 is a ten-times-scale vertical section through the phototube and A-scope face. It shows the optical paths and relative position of the photocathode in relation to the slit and beam spot. Two beam positions are drawn in the locations where the photocurrent has fallen to 50% of the on-axis value. The distance between these half-amplitude positions may be taken as a measure of the unit resolution, Δy. This distance is 3 mm in the equipment when a 1 mm spot diameter and 1 mm slit are employed. With a signal height $Y = 120$ mm and $\Delta y = 3$ mm we may thus obtain a peak resolution index $R_p = 40$.

A study of Fig. 5 will show that no great improvement in resolution may be obtained by withdrawing the phototube and employing a second slit without a considerable reduction in illumination and photocurrent signal. It is also clear that further reduction of the slit height will make only a slight improvement in resolution.

Attempts to increase resolution which reduce illumination will require a more intense spot. As beam intensity is increased the spot diameter is also increased, and the unit resolution increases. The drawing shows a spot diameter of one mm which was optimum in most cases.

An effective but impractical method of improving the resolution is to place the slit inside the CR tube. Although impractical, the unit resolution could be reduced to 1 mm or less by this method. A practical method for doing this is described in Section 8.

FIG. 5

OPTICAL DETAILS OF ANALYZER.
SCALE 10 X FULL SIZE

7. RESULTS

To illustrate different types of incremental-distribution-density functions, the results of analyzing two different noise sources are presented.

Figure 6A shows the noise as it appears on the face of the A-scope from noise source No. 1. From top to bottom, the noise is shown with positive, negative and no clipping. Fig. 6B shows the $p_{\Delta}(y)$ for the central and bottom distributions of Fig. 6A. It is noted that the unclipped distribution density is approximately Gaussian, but a severe horn is developed in the $p_{\Delta}(y)$ for negative clipping. The central pulse was obtained by a no-signal scan, giving a measure of the unit resolution.

Figure 7 shows $p_{\Delta}(y)$ for noise source No. 1 with different arrangements of clipping. Oscillogram A is for no clipping. The following three are for positive clipping, negative clipping, and both positive and negative clipping in that order. The difference between Fig. 6B and Fig. 7 is that a smaller vertical gain is employed in the D-scope for Fig. 7. Other conditions are the same.

Figure 7D shows that for this clipping arrangement, the distribution density is affected at the center as well as at the sides producing a bimodal curve.

Figure 8 shows a similar set of $p_{\Delta}(y)$ curves for noise source No. 2. It is noted that the distribution density in Fig. 8A is assymetric with no clipping, because of a peculiarity of the circuit in this source. When positive and negative clipping was used, Fig. 8D, the clipping action was quite different, and a single peaked curve was obtained.

Noise source No. 1 employed a 931-A multiplier phototube as the noise generator. Source No. 2 employed a 6D4 gas triode operating in a magnetic field,

A.

B.

FIG. 6

NOISE AND ITS DISTRIBUTION DENSITY.

NOISE SOURCE NO. 1.

FIG. 7

ANALYSIS OF NOISE SOURCE NO. 1.

A. NO CLIPPING
B. POSITIVE CLIPPING
C. NEGATIVE CLIPPING
D. BOTH POSITIVE AND NEGATIVE CLIPPING

M-970 A-P4-17 JEM 10-9-53

FIG. 8

ANALYSIS OF NOISE SOURCE NO. 2.

A. NO CLIPPING
B. POSITIVE CLIPPING
C. NEGATIVE CLIPPING
D. BOTH POSITIVE AND NEGATIVE CLIPPING

followed by equalizing circuits to flatten the noise spectrum in the range 100 kc to 10 mc. The difference in distribution densities for the two noise sources is clearly evident. The different clipping action arose from the difference in distribution densities, and from a difference in power level at the clipper stage.

8. MODIFIED EQUIPMENT

By modifying the optical system, it is possible to decrease the unit resolution to less than one mm. This requires that an image of the A-scope screen be formed by a high quality, color-corrected camera lens, and a carefully made slit properly placed in the focal plane. It is now possible to locate the slit and image in the same plane, and thus achieve the resulting reduction of Δy mentioned at the end of Section 6.

An ideal arrangement is shown in Fig. 9. A Land Polaroid camera is employed with the A-scope. The focal plane is horizontal, and the slit and photocell are mounted above in a light-tight housing. This has the additional advantage that the entire image on the A-scope may be examined through the viewing tube before and during analysis. This is possible because the dichroic mirror of the Polaroid camera reflects most of the energy below 5000 Å into the lens and photocell system, but transmits a portion of the light above 5000 Å for visual observation.

Using a 200 micron slit and a 0.5 mm spot diameter, it should be possible to obtain a unit resolution of less than one mm measured at the tube face. A peak resolution index of 120 or more can then be realized.

The average maximum light entering the slit in this system will be of the order of a few microlumens instead of one millilumen. The 1P42 having

M-970 A-S4-51 JEM 10-8-53

FIG. 9

MODIFIED ANALYZER.

a sensitivity of only 30 x 10^{-6} amps per lumen is no longer of any use and we must employ a multiplier phototube such as the 931-A or the 1P28. When operated at 90 volts per stage, these tubes have sensitivities of approx. 10 amperes per lumen. For accurate work, the phototube must be powered by a well regulated 1000 volt power source. If a regulated power supply is employed, it will be convenient to make the voltage adjustable, since this gives excellent control of the tube sensitivity. If batteries are employed, they must be enclosed in a well-grounded shield to prevent electrostatic pickup.

The multiplier phototube fatigues rather badly at high anode currents, and therefore the maximum average anode current should not exceed 100 microamps. The average dark current for a group of 10 RCA Type 1P28 tubes was 2 x 10^{-9} amperes,[1] so that no trouble is experienced from this cause. The tube noise due to photocurrent[2] is a function of the bandwidth Δf. Since the bandwidth will be limited to a few cycles per second by the integrating capacitor C_y, the noise level will be negligible.

Because of the great sensitivity of the multiplier phototube, it is possible to work the A-scope with less intensity, which insures further that the conditions described in Section 3.1 will be fulfilled. Two additional advantages are obtained. First,a less intense spot may be focussed to a smaller diameter. Second, a smaller slit width may be employed. Both of these lead to better resolution provided the slit is adjusted exactly in the focal plane. Stopping down the lens will make this adjustment less critical.

This modified set-up will have greater accuracy and better resolution but requires that the sharp-edged slit jaws be machined accurately, and that all adjustments be made with extreme care.

---

1 Orr, L. W., "A Study of the High Frequency Structure of Spectral Light Intensity Produced by Spark Excitation Using Electron Multiplier Phototubes," Doctoral Thesis, Univ. of Mich.,Ann Arbor, Mich., 1949, p. 45.

2 Ibid.,p. 46

9. CONCLUSION

The accuracy of the method may be judged by comparing the calculated distribution density of a known source with the observed, as in Fig. 2. The sinusoid is a good test-case for accuracy because of the large variation in the density function. When enlargements of Figs. 2A and 2B are superimposed, it is found that the two curves are almost identical except at the horns of the distribution. The observed horns are neither as sharp nor as high as the calculated ones. This is due to the shape of the resolution pulse, (center of Fig. 2B), which is clearly not rectangular. It was implicitly assumed in calculation that the resolution pulse was rectangular (Eq 6).

For Gaussian-like distributions (Fig. 7A) the relative error is quite small in the central region, but increases near the tails of the distribution because of inaccuracies due to dc drift, small dimensions and finite width of trace. This type of error may be overcome by re-scanning with increased A-scope intensity, and increased D-scope gain. Although the central distribution will generally go off-scale, the tails of the distribution will be presented with greatly reduced error.

Errors are larger for situations like the horns in Fig. 2 because of the reason stated above. This may be overcome to a great extent by increasing the resolution as outlined in Section 8. The overall accuracy of the minimum set-up is estimated at about 5%, but is better than this in many cases.

Considering the simplicity and low cost of the set-up, its broad-band capabilities up to 500 mc and its speed of analysis, the method is surprisingly accurate and versatile, and its performance at this laboratory has been most gratifying.

DISTRIBUTION LIST

1 copy	Director, Electronic Research Laboratory Stanford University Stanford, California Attn: Dean Fred Terman
1 copy	Commanding Officer Signal Corps Electronic Warfare Center Fort Monmouth, New Jersey
1 copy	Chief, Engineering and Technical Division Office of the Chief Signal Officer Department of the Army Washington 25, D. C. Attn: SIGGE-C
1 copy	Chief, Plans and Operations Division Office of the Chief Signal Officer Washington 25, D. C. Attn: SIGOP-5
1 copy	Countermeasures Laboratory Gilfillan Brothers, Inc. 1815 Venice Blvd. Los Angeles 6, California
1 copy	Commanding Officer White Sands Signal Corps Agency White Sands Proving Ground Las Cruces, New Mexico Attn: SIGWS-CM
1 copy	Signal Corps Resident Engineer Electronic Defense Laboratory P. O. Box 205 Mountain View, California Attn: F. W. Morris, Jr.
75 copies	Transportation Officer, SCEL Evans Signal Laboratory Building No. 42, Belmar, New Jersey For - Signal Property Officer Inspect at Destination File No. 25052-PH-51-91(1443)

1 copy	W. G. Dow, Professor Dept. of Electrical Engineering University of Michigan Ann Arbor, Michigan
1 copy	H. W. Welch, Jr. Engineering Research Institute University of Michigan Ann Arbor, Michigan
1 copy	Document Room Willow Run Research Center University of Michigan Willow Run, Michigan
10 copies	Electronic Defense Group Project File University of Michigan Ann Arbor, Michigan
1 copy	Engineering Research Institute Project File University of Michigan Ann Arbor, Michigan